

# First Principles Studies of Vanadia–Titania Monolayer Catalysts: Mechanisms of NO Selective Reduction

Andrea Vittadini\*

CNR-ISTM and INSTM, Chemistry Department, University of Padova, via Marzolo 1, I-35131 Padova, Italy

Maurizio Casarin

INSTM and Chemistry Department, University of Padova, via Marzolo 1, I-35131 Padova, Italy

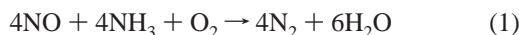
Annabella Selloni

Chemistry Department, Princeton University, Princeton, New Jersey 08540

Received: November 17, 2004; In Final Form: December 21, 2004

The selective reduction of NO with NH<sub>3</sub> catalyzed by isolated VO<sub>x</sub> species grafted onto TiO<sub>2</sub> (anatase) is studied by means of periodic density functional calculations. NH<sub>3</sub> is adsorbed molecularly by the bare support both as a Lewis-bonded complex at (101) 5-fold coordinated Ti sites, and as a H-bonded complex at (001) Ti–OH sites. Analogous interactions are predicted for stable submonolayer VO<sub>x</sub> species, which provide V<sup>5+</sup> Lewis acid sites and V–OH sites. Neither Ti–OH nor submonolayer V–OH groups act as Brønsted acids toward NH<sub>3</sub>. Reaction pathways where both Lewis-bonded and H-bonded NH<sub>3</sub> complexes yield a NH<sub>2</sub>NO intermediate are found. In the former case, a (rate-determining) deprotonation step of NH<sub>3</sub> is required, whereas, in the latter, NH<sub>2</sub>NO is formed directly through a concerted mechanism. This suggests that many channels may contribute to the NO reduction process.

Vanadia–titania systems are active for a number of reactions, particularly for the selective catalytic reduction (SCR) of NO (DeNO<sub>x</sub> process):<sup>1</sup>



Experiments show that, at variance with NO, NH<sub>3</sub> significantly interacts with both the titania support and the vanadia overlayer.<sup>1</sup> However, understanding the chemistry of NH<sub>3</sub> on vanadia–titania catalysts, and its role in the SCR process is difficult, because of the heterogeneity of the system. In fact, different vanadia phases are believed to be present in the catalyst:<sup>2,3</sup> a monolayer strongly and directly attached to the support, an amorphous phase in close contact with the monolayer, and for high vanadia loadings, V<sub>2</sub>O<sub>5</sub> crystals. Furthermore, the support is not uniformly covered (i.e., part of the TiO<sub>2</sub> surface is also exposed), even for the highest loadings.

Although difficulties in modeling the structure of amorphous vanadia have so far hampered the theoretical investigation of this phase, crystalline vanadia, and its interaction with NH<sub>3</sub>, has been studied theoretically by several authors.<sup>4–6</sup> These studies indicate that NH<sub>3</sub> adsorption onto V–OH groups present as defects at the V<sub>2</sub>O<sub>5</sub>(010) surface leads to strongly bound (~1.1 eV) NH<sub>4</sub><sup>+</sup> species.<sup>5</sup> More recent calculations further predict that these defects can catalyze NO reduction, with an activation energy of ~0.5 eV.<sup>6</sup>

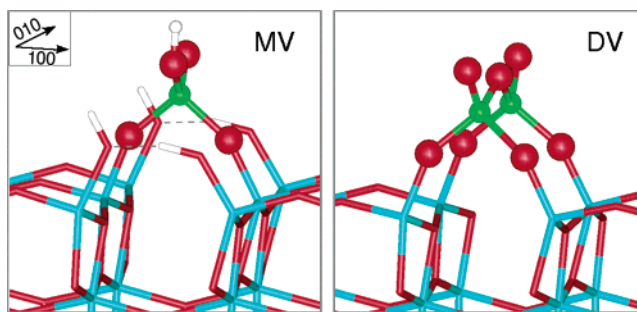


**Figure 1.** Schematic representation of tetrahedral submonolayer monomeric (MV) and dimeric (DV) vanadate units, as determined in ref 9. Note that the units replace OH pairs, which in turn result from the dissociation of H<sub>2</sub>O molecules on O bridges of the anatase (001) surface. The overlayer and the support are depicted in a ball-and-stick and in a “licorice” style, respectively. H atoms are white, V green, O red, and Ti blue.

Over the past few years, accurate theoretical studies of the monolayer phase have also become available.<sup>7–9</sup> In particular, our calculations<sup>9</sup> indicate that at low V-coverages monovanadate (MV) and divanadate (DV) tetrahedral species (see Figure 1) are energetically favored, in agreement with the experiment.<sup>2</sup>

In the present paper, we want to focus on such tetrahedral submonolayer species, with the aim of understanding whether they could play a role in the SCR process.

Unlike previous theoretical investigations, which have been carried out using either semiempirical calculations,<sup>10,11</sup> or small gas-phase cluster models of the catalyst,<sup>7</sup> reaction pathways have

\* Corresponding author. Fax: +39-049-8275161. E-mail: andrea.vittadini@unipd.it.

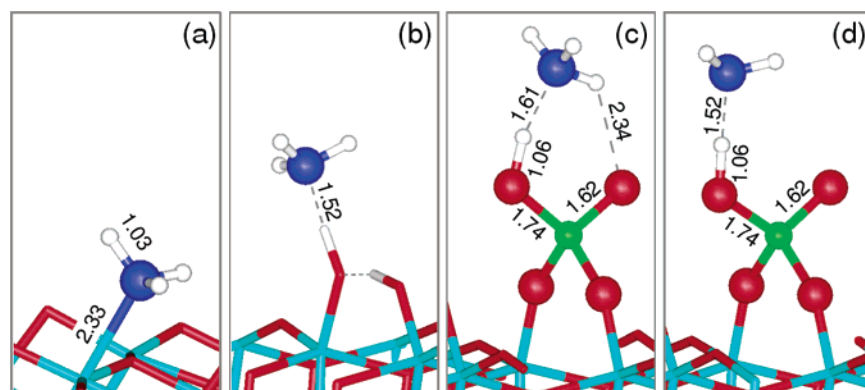
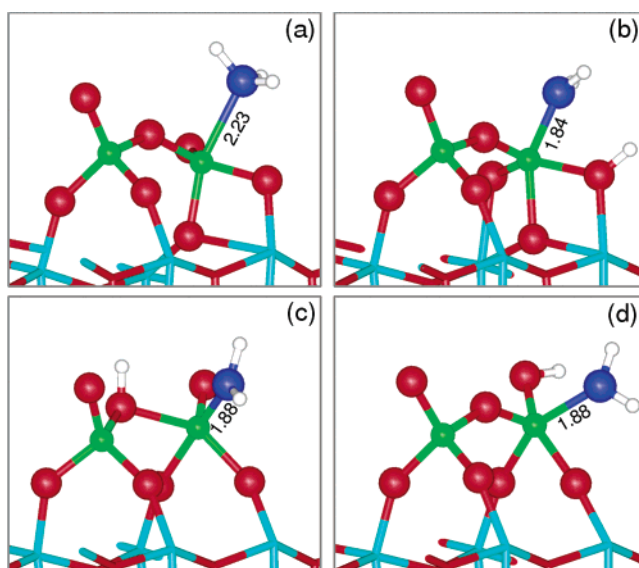


**Figure 2.** Equilibrium configurations for  $\text{NH}_3$  adsorbed on (a)  $\text{Ti}^{4+}$  Lewis acid sites of the (101) surface, (b)  $\text{Ti}-\text{OH}$  sites of the hydroxylated (001) surface, (c)  $\text{V}-\text{OH}$  site of MV species in a bridge configuration, and (d) the same, in a terminal configuration. The vanadia-titania system is represented as in Figure 1. Adsorbates are shown in a ball-and-stick style; N atoms are colored dark blue. Displayed distances are in Å. Internal  $\text{NH}_3$  bonds change by less than 0.005 Å.

been here searched by coupling density functional theory (DFT) and periodically repeated models. This combined approach allows us to perform accurate total energy calculations for minima and saddle points on realistic surface models. Plane-wave DFT calculations have been performed using both a Car-Parrinello code, as described in ref 12, and the PWSCF 2.0 code.<sup>13,14</sup> The PBE<sup>15</sup> functional has been used to describe non local exchange and correlation effects. “Ultra-soft” relativistic pseudopotentials<sup>16</sup> have been adopted, with small ion cores, including the 1s state for O and N, and the 1s, 2s, and 2p states for Ti and V. The smooth part of the wave functions was expanded in plane waves with a kinetic energy cutoff of 25 Ry, whereas the cutoff for the augmented electron density was 200 Ry. The surface Brillouin zone was sampled at the  $\Gamma$  point. As in ref 9, the  $\text{TiO}_2$  (anatase) support is assumed to expose (101) surfaces and minority hydroxylated (001) surfaces, onto which  $\text{VO}_x$  species are grafted. The theoretical<sup>17</sup> lattice constants were used. Atomic relaxations were carried out until residual forces were less than 0.05 eV/Å. Vanadia species and reactant/adsorbate molecules were introduced only on the upper part of the slabs. Transition states (TS) were searched with the “climbing-image nudged elastic band” (CI-NEB) algorithm,<sup>18</sup> and by constrained minimizations. Vibrational analyses were not carried out.

**$\text{NH}_3$  Interaction with Intrinsic  $\text{TiO}_2$  Sites.** We first consider the interaction of  $\text{NH}_3$  with the reactive sites of the support. On the basis of our previous work on anatase surfaces,<sup>9,17,19</sup> these are expected to be the 5-fold coordinated cations exposed at the (101) surface and the OH groups present at the (001) surface. Adsorption energies ( $E_{\text{ads}}$ ) are 0.92 eV in the former case (Figure 2a) and 0.68 eV in the latter (Figure 2b). In both cases,  $\text{NH}_3$  adsorption complexes are similar to  $\text{H}_2\text{O}$  ones, but more stable. In fact, we obtain  $E_{\text{ads}} = 0.92$  and 0.68 eV for  $\text{NH}_3$  vs  $E_{\text{ads}} = 0.74$  and 0.58 eV for  $\text{H}_2\text{O}$ ,<sup>19</sup> on the (101) and (001) surfaces, respectively. Furthermore (see Figure 2b),  $\text{NH}_3$  is *not* protonated by anatase hydroxyls, in agreement with experiments which show no Brønsted acidity for pure anatase.<sup>20,21</sup>

**$\text{NH}_3$  Interaction with Submonolayer  $\text{VO}_x$  Species.** We considered as possible adsorption sites undercoordinated  $\text{V}^{5+}$  centers, present in both MV and DV units, and  $\text{V}-\text{OH}$  centers, carried by MV units.<sup>9</sup> We found that  $\text{NH}_3$  can interact with  $\text{V}-\text{OH}$  centers either in a *bridging* or in a *terminal* configuration (see Figure 2c,d). The bridging geometry is favored by  $\sim 0.2$  eV, and its structure is *asymmetric*; i.e., the OH groups carried by MV species are unable to produce ammonium ions (see



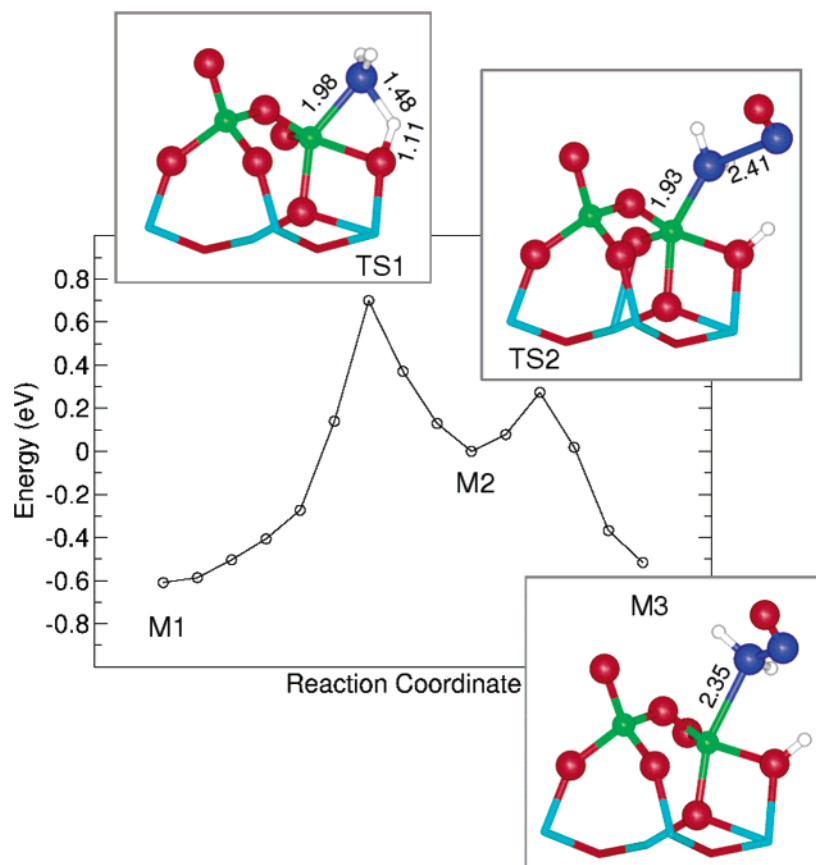
**Figure 3.** Equilibrium configurations for (a)  $\text{NH}_3$  molecularly adsorbed at a DV and (b)–(d)  $\text{NH}_3$  dissociatively adsorbed at a DV. These configurations differ by the O site at which the proton is attached, which are (b)  $\text{V}-\text{O}-\text{Ti}$ , (c)  $\text{V}-\text{O}-\text{V}$ , and (d)  $\text{V}=\text{O}$ .

Figure 2c). This agrees with the experimental observation that monolayer catalysts have a reduced protonating power toward  $\text{NH}_3$ .<sup>22</sup> The adsorption energy is 0.60 eV, which is in the lower part of the 0.7–1.1 eV experimental range.<sup>23,24</sup> MV units belonging to polyvanadate chains and those directly grafted to the support are found to behave almost identically (differences are smaller than 0.1 eV for energies, and 0.1 Å for bond distances).

The interaction with  $\text{V}^{5+}$  Lewis acid sites has been studied for DV units.

Despite the structural differences, the bonding energy of the resulting complex (0.61 eV) is, most likely accidentally, identical to that computed for  $\text{NH}_3$  H-bonded to  $\text{V}-\text{OH}$  centers. Unlike that case, however, the interacting  $\text{VO}_x$  species undergoes large modifications (see Figure 3a): the symmetry of the DV unit is lost, the  $\text{V}=\text{O}$  group becomes almost parallel to the surface, and one of the O connecting V to the support is moved back to the bridging position, as in the unreconstructed clean surface.

**Catalytic Reduction of NO:  $\text{V}^{5+}$  Lewis Acid Sites.** We now want to assess whether submonolayer tetrahedral species can catalyze the NO reduction. Ramis et al.<sup>21</sup> suggested that a possible mechanism (known as “amide-nitrosamide” mecha-



**Figure 4.** Potential energy (PE) profile for the first steps of the SCR process at a Lewis acidic site as obtained by DFT CI-NEB calculations. Each point corresponds to a NEB image. Solid line is only a guide to the eye. TS1 and TS2 were obtained in separate calculations, and the two PE curves were merged at M2. Structures of M1 and M2 are shown in Figure 3a,b, respectively. Other structures are shown in the insets. Energies are referred to the bare DV unit and gas-phase adsorbates.

nism) implies the partial deprotonation of a Lewis-bonded  $\text{NH}_3$  molecule. The  $-\text{NH}_2$  (amide) group formed in this way is then attacked by an incoming or weakly adsorbed NO, forming a  $\text{NH}_2\text{NO}$  (nitrosamide) intermediate. This is finally decomposed to  $\text{N}_2$  and  $\text{H}_2\text{O}$ , whereas the catalyst is reoxidized by gas-phase  $\text{O}_2$  molecules.

To model the first step of the above-described process, we first computed the energy of the possible structures obtained by transferring a proton from the DV- $\text{NH}_3$  complex of Figure 3a to one of the DV O atoms, viz.: the V-O-Ti site (Figure 3b,  $E_{\text{ads}} = -0.02$  eV); the V-O-V site (Figure 3c,  $E_{\text{ads}} = 1.13$  eV); the V=O site (Figure 3d,  $E_{\text{ads}} = 0.08$  eV). Thus, the V-O-V bridging oxygen site is highly unfavored, whereas the other ones give intermediates of comparable stability.<sup>25</sup> Because of the rather small lateral size of our slab model, however, significant interactions between consecutive images of the DV- $\text{NH}_3$  complex occur when H is adsorbed at V=O (H can form an hydrogen bond with the V=O at the other end of the DV unit). Therefore, we limited our investigation to reaction pathways involving the V-O-Ti site. The TS for the  $\text{NH}_3$  deprotonation was searched with the CI-NEB algorithm, by using 10 images. The resulting reaction path corresponds to the M1  $\rightarrow$  M2 part of the curve reported in Figure 4 and gives an activation energy of 0.7 eV.

In the second reaction step (M2  $\rightarrow$  M3), we considered a gas-phase NO molecule approaching the  $-\text{NH}_2$  group. The resulting product is a  $\text{NH}_2\text{NO}$  species molecularly adsorbed at the Lewis acid site. The computed barrier of this second step ( $\sim 0.2$  eV) is much lower than the first one, which is thus rate

determining. Altogether, our calculations yield a 0.7 eV barrier<sup>26</sup> for the SCR at DV species, which is compatible with the experimental value of 0.4–0.9 eV.<sup>27</sup>

**Catalytic Reduction of NO: V-OH Sites.** A modified version of the amide-nitrosamide mechanism was proposed by Topsøe et al.,<sup>28,29</sup> where NO attacks a  $\text{NH}_3$  molecule that is interacting with a V-OH and a V=O group simultaneously. The products are then obtained by passing through some unstable intermediate. We examined the possibility that a similar mechanism occurs at a MV unit, where V=O and V-OH functions are carried by the same V atom.<sup>30</sup> In this case we used a constrained minimization approach where the reaction coordinate was the N-N distance between the gas-phase NO and the adsorbed  $\text{NH}_3$  molecules.<sup>31</sup> We found that at a N-N distance of 1.74 Å the total energy is maximized, and the forces acting on the N atoms are vanishingly low, which is indicative of a saddle point. To substantiate this evidence, we ran unconstrained molecular dynamics simulations starting from two configurations where the N-N distance was changed by  $\pm 0.01$  Å with respect to the presumed saddle point value of 1.74 Å.

The resulting trajectories (see Figure 5) evolve toward the reactants ( $\text{NO} + \text{NH}_3$ ) and the intermediate product ( $\text{NH}_2\text{NO}$ ), which confirms the constrained minimization result. Interestingly, our results indicate that the formation of a  $\text{NH}_3\text{NO}$  adduct as in the originally proposed mechanism<sup>28</sup> is not required, whereas the same  $\text{NH}_2\text{NO}$  intermediate of the amide-nitrosamide mechanism is readily formed via a concerted process. Furthermore, the two mechanisms involve similar energy barriers (0.7 vs 0.6 eV). Hence, we conclude that, on the grounds of

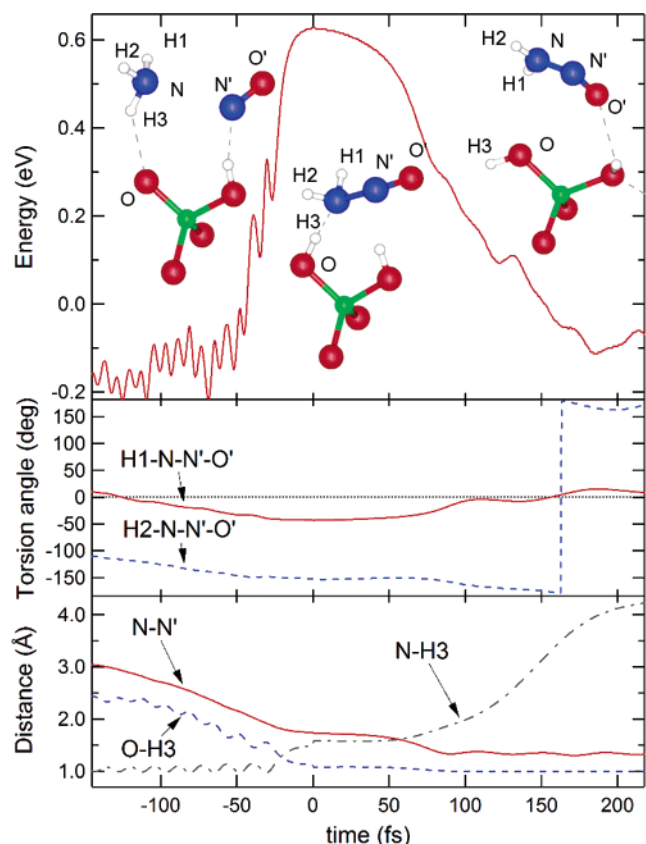


**Figure 5.** Molecular dynamics trajectories obtained by starting from configurations before (left part, with negative time values) and after the TS (right part) for the SCR process occurring at a V—OH site carried by a MV species. Starting configurations have N—N distances of 1.73, and 1.75 Å, respectively. Top panel: evolution of the total energy, referred to a bare MV unit and gas-phase adsorbates. Insets show the structures of the TS, and of the final points of the backward and forward trajectories. Middle and bottom panels: evolution of relevant torsion angles and distances. Atom codes are explained in the top panel insets.

energetics, both  $V^{5+}$  and V—OH sites associated to tetrahedral submonolayer species are able to catalyze the NO reduction. Furthermore, the two reaction mechanisms are more similar than expected, involving the formation of the same  $NH_2NO$  intermediate. Last, none of these mechanisms requires the formation of  $NH_4^+$ , which agrees with the finding that several systems where Brønsted acidity is absent are nonetheless SCR active.<sup>1</sup>

In summary, our DFT calculations show that, on the bare anatase support,  $NH_3$  is more tightly bound to the  $Ti^{5+}$  sites present at the (101) facets, than to the Ti—OH centers present at the (001) ones. Furthermore,  $NH_3$  is not protonated either by these OH groups or by those carried by submonolayer tetrahedral monovanadate species, which are grafted on the same (001) facets. Last, it is shown that submonolayer  $VO_x$  species are able to catalyze the NO reduction. Mechanisms involving both Lewis-bonded and hydrogen-bonded  $NH_3$  isoenergetic species are viable, which suggests that structural requirements for the active sites could be rather loose.

**Acknowledgment.** All the calculation reported in this work have been performed at the Keck Materials Science Computing Center of the Princeton Materials Institute.

## References and Notes

- (1) Busca, G.; Lietti, L.; Ramis, G.; Berti, F. *Appl. Catal. B. Environ.* **1998**, *18*, 1.
- (2) Grzybowska-Świerkosz, B. *Appl. Catal. A. Gen.* **1997**, *157*, 263.
- (3) Bond, G. C. *Appl. Catal. A. Gen.* **1997**, *157*, 91.
- (4) Keller, D. E.; Weckhuysen, B. M. *Catal. Today* **2003**, *281*, 1.
- (5) Yin, X.; Han, H.; Gunji, I.; Endou, A.; Ammal, S. S. C.; Kubo, M.; Miyamoto, A. *J. Phys. Chem. B* **1999**, *103*, 4701.
- (6) Yin, X.; Han, H.; Miyamoto, A. *Phys. Chem. Chem. Phys.* **2000**, *2*, 4243.
- (7) Gilardoni, F.; Weber, J.; Baiker, A. *J. Phys. Chem. A* **1997**, *101*, 6069.
- (8) Anstrom, M.; Dumesic, J. A.; Topsøe, N. Y. *Catal. Lett.* **2002**, *78*, 281.
- (9) Anstrom, M.; Topsøe, N. Y.; Dumesic, J. A. *J. Catal.* **2003**, *213*, 115.
- (10) Calatayud M.; Mguig, B.; Minot, C. *Surf. Sci. Rep.* **2004**, *169*, 169 and references therein.
- (11) Calatayud M.; Minot, C. *J. Phys. Chem. B* **2004**, *108*, 15679.
- (12) Vittadini, A.; Selloni, A. *J. Phys. Chem. B* **2004**, *108*, 7337.
- (13) Jug, K.; Homann, T.; Bredow, T. *J. Phys. Chem. A* **2004**, *108*, 2966.
- (14) According to the results of ref 10, all TS are below the energy level of the separate reactants. This implies an overall zero-energy barrier, which disagrees with the experiment.
- (15) Car, R.; Parrinello, M. *Phys. Rev. Lett.* **1985**, *55*, 2741.
- (16) Laasonen, K.; Pasquarello, A.; Car, R.; Lee, C.; Vanderbilt, D. *Phys. Rev. B* **1993**, *47*, 10142.
- (17) Baroni, S.; Dal Corso, A.; de Gironcoli, S.; Giannozzi, P. <http://www.pwscf.org>.
- (18) Both codes were recently bundled in the “espresso” suite.<sup>13</sup>
- (19) Perdew, J. P.; Burke, K.; Ernzerhof, M. *Phys. Rev. Lett.* **1996**, *77*, 3865.
- (20) Vanderbilt, D. *Phys. Rev. B* **1990**, *41*, 7892.
- (21) Lazzeri, M.; Vittadini, A.; Selloni, A. *Phys. Rev. B* **2001**, *63*, 155409.
- (22) Henkelman, G.; Uberuaga, B. P.; Jónsson, H. *J. Chem. Phys.* **2000**, *113*, 9901.
- (23) Henkelman, G.; Jónsson, H. *J. Chem. Phys.* **2000**, *113*, 9978.
- (24) Vittadini, A.; Selloni, A.; Rotzinger, F. P.; Grätzel, M. *Phys. Rev. Lett.* **1998**, *81*, 2954.
- (25) Busca, G.; Saussey, H.; Saur, O.; Lavalley, J. C.; Lorenzelli, V. *Appl. Catal.* **1990**, *14*, 243.
- (26) Ramis, G.; Busca, G.; Lorenzelli, V.; Forzatti, P. *Appl. Catal.* **1990**, *64*, 243.
- (27) Borovkov, V. Yu.; Mikheeva, E. P.; Zhidomirov, G. M.; Lapina, O. B. *Kinet. Catal.* **2003**, *44*, 710.
- (28) Srnak, T. Z.; Dumesic, J. A.; Clausen, B. S.; Tornquist, E.; Topsøe, N. Y. *J. Catal.* **1992**, *135*, 246.
- (29) Our value is lower with respect to previous estimates based on cluster models (1.16–1.33 eV<sup>10</sup> and 0.88 eV<sup>22</sup>). These discrepancies are difficult to analyze because there are also differences both in the structural details of the models, and in the theoretical approaches.
- (30) A high reactivity of the V—O—Ti site was also computed in ref 8.
- (31) We assume that the steps involving the  $NH_2NO$  decomposition and the catalyst reoxidation involve low energy barriers, as suggested by the experiment.<sup>1</sup>
- (32) Nova, I.; Lietti, L.; Tronconi, E.; Forzatti, P. *Chem. Eng. Sci.* **2001**, *56*, 1229.
- (33) Wong, W. C.; Nobe, K. *Ind. Eng. Chem. Prod. Res. Dev.* **1984**, *23*, 564.
- (34) Marshneva, V. I.; Slavinskaya, E. M.; Kalinkina, O. V.; Odegova, G. V.; Moroz, E. M.; Lavrova, G. V.; Salanov, A. N. *J. Catal.* **1995**, *124*, 171.
- (35) Topsøe, N.-Y., *Science* **1994**, *265*, 1217.
- (36) Dumesic, J. A.; Topsøe, N.-Y.; Topsøe, H.; Chen, Y.; Slabaiak, T. *J. Catal.* **1996**, *163*, 409.
- (37) In the mechanism proposed in refs 28 and 29, the V=O and V—OH functions are provided by distinct surface sites.
- (38) We were not able to obtain a converged CI-NEB pathway in which the starting state was a NO approaching an adsorbed  $NH_3$ , and the final state was adsorbed  $NH_2NO$ .